The significance of loading profile on the occlusion mechanics of a viscoelastic periodontal ligament analogue-supported tooth

James P. Thompson, Thomas R. Katona and George J. Eckert

ABSTRACT

Background: Benchtop studies of occlusal contact forces have used teeth that were rigidly attached or supported by readily available viscoelastic (VE) materials that served as periodontal ligament (PDL) substitutes. More recent specimens have incorporated a precisely dimensioned VE PDL-behavior matched analogue.

Objectives: The objectives of this study were to evaluate a modified loading protocol (step function) that is more appropriate to VE support than the previously used ramp function. The occlusion manifestations of the time-dependent behaviors (*creep* and *recovery*) of the PDL analogue were examined using the revised protocol.

Methods: A mandibular 1st molar denture tooth was set into a precision-machined root/socket assembly. The PDL substitute was then cured to tight dimensional tolerances. The matching rigidly fixed maxillary denture tooth was aligned into a Class I centric molar relationship in a testing apparatus. The weighted maxillary assembly was then cycled onto and off of the load cell-supported mandibular assembly. For statistical purposes, three loading schedules were tested in 21 0.05 mm shifted occlusal relationships. Rigid attachment served as control.

Results: Statistical analyses were performed on the peak values of $F_{lateral}$, the net in-occlusal plane force component of the occlusal contact forces. It was found that there were statistically significant differences between: chomp-to-chomp ($p < .038$), PDL vs. rigid ($p < .001$) and loading schedules ($p < .044$ for PDL only).

Conclusion: The loading protocol affects outcomes, and the step functions maintained consistent timing with prescribable creep and recovery periods.

Keywords: Occlusion; Periodontal ligament; Viscoelasticity; Loading

Introduction

A series of benchtop studies on the forces acting on occluding single (denture, ceramic and stainless-steel) teeth and full-arch dentiforms had been performed, with and without occlusion detection products and/or (human or various artificial) salivas.(Helms, Katona et al. 2012, McCrea, Katona et al. 2015, Mitchem, Katona et al. 2017, Beninati and Katona 2019) The focus of those studies was on the periodontium-damaging in-occlusal plane force component (**$F_{lateral}$**) produced by the occlusal contacts.(Dawson 2006, Harrel and Nunn 2009, Okeson 2013, Passanezi and Sant'Ana 2019, Yang and Chung 2019) The overall results were that during a complete bite cycle (a chomp), the **$F_{lateral}$** force vector magnitudes and directions are transitory and disclusion (vs. occlusion) tends to produce higher magnitudes.

In those studies, the teeth were rigidly attached in the testing apparatus (*i.e.*, mimicking ankylosis and implant support). To improve model verisimilitude, a viscoelastic (VE) periodontal ligament (PDL) analogue (Xia and Chen 2013) was precision incorporated into a subsequent experiment in which the impact of the PDL was assessed.(deMoya, Schmidt et al. 2021) The PDL, as all biological tissues (except tooth enamel) are viscoelastic materials.(ScienceDirect 2019a, ScienceDirect 2019b) Although the key overall conclusions and observations with the PDL and rigid specimens were similar, the nuances were very different. Thus, it was concluded that in most, but not all, occlusion studies, it would be prudent to include the difficult, time-consuming, and expensive PDL modification.

The primary effects of the PDL analogue in these tests are through its VE time-dependent behaviors, *creep* and *recovery*. In practical terms, *creep* refers to the continuous change in the dimensions of the material while a constant load is applied to it. *Recovery* refers to the tendency of the structure to return towards its original, pre-loaded, dimensions after the load is removed. Both phenomena are time-depended, meaning that the amount of deformation during creep depends on the duration of load application, and the amount of recovery depends on the length of time that the load has been removed.

The rigid specimen studies had been conducted with a ramp displacement loading profile. However, because of the VE time-factor, ramp loading became an issue with the PDL. Thus, the purpose of this study was to better elucidate the manifestations of the VE behavior in occlusal contact mechanics by modifications in the established loading protocols, thereby controlling the prescription and control of VE *creep* and *recovery*. Essentially, the previously applied ramp displacement loading profile was replaced by a step function.

Methods and Materials

Brief description

Two opposing molar denture teeth were mounted in a testing apparatus (**Fig. 1**) and set into occlusion. The weighted maxillary tooth was lowered and raised in a prescribed step

displacement profile. A load cell continuously recorded the forces experienced by the mandibular tooth that was attached rigidly or with the PDL analogue. Except for the step loading profile, the protocol is essentially that of the previous ramp loading study.(deMoya, Schmidt et al. 2021)

Testing apparatus

The testing apparatus, **Figs. 1A** and **B**, consisted of a weighted (~20 N) maxillary tooth assembly that was carried by a pair of vertical precision slides (Mini-Guide, Double Carriage, Model #SEBS 9BUU2-275, Nippon Bearing Co, Ojiya, Japan). In the lower assembly, the mandibular tooth was supported by a load cell (Gamma transducer SI-65-5, ATI Industrial Automation, (Apex, NC, USA) that continuously measured (at 100 Hz) force components F_x, F_y and F_z (0 - 65 ± 0.0125 N), **Fig. 1C**. The entire unit was bolted onto a mechanical testing machine (MTS Bionix 858, MTS Corporation, Minneapolis, MN, USA) that was used to raise and lower the maxillary assembly with a (Zinc Plated Steel Sash #35, Everbilt, Atlanta, GA, USA) sash chain. The load cell output was recorded by a laptop computer (Dell Inspiron 15R-5537, Dell Corporation, Round Rock, TX, USA) using NI-DAQmx software (National Instruments Corporation, Austin, TX, USA).

Specimen preparation

The maxillary crown holder (**Fig. 1D**, left) is a precision machined (10 x 10 x 28 mm) aluminum bar with a large diameter cylindrical hole to receive the denture tooth in one end and a threaded mounting hole in the other. The similarly dimensioned mandibular crown holder (**Figs. 1D** center and right) consists of a "tooth" with a conical root and a precisely matching socket. Their dimensions were calculated such that a 1.0 mm gap between the "CEJ" and the bone crest produces a 0.30 mm thick PDL space, **Fig. 1E**.

Maxillary and mandibular right first molar denture teeth (Dentsply Portrait IPN 33°, York, PA, USA) were trimmed to fit into their aluminum cylindrical recesses. Retentive dimples were placed in the aluminum and notches were cut in the denture tooth bases. The maxillary crown was attached with (Dentsply Caulk, Dentsply International, Milford, DE, USA) orthodontic resin. For assembly purposes, the 2 mandibular parts were taped (generic cellophane tape) together without a gap between them. The upper assembly was affixed to the testing instrument, while the taped-together mandibular part, in its mounting plate, sat loosely on the instrument's table. The mandibular cylindrical recess was ~¾ filled with orthodontic resin. Then, the denture tooth was placed into the lightly cured resin, the unweighted upper assembly was lowered gently into occlusal contact, the lower assembly was situated into a Class I molar relationship, and the resin was allowed to fully cure. Once cured, the cellophane tape was removed.

The PDL analogue was mixed according to the specifications (Xia and Chen 2013) as a 50 - 50% mixture of gasket sealant No. 2 (GS) and RTV 587 silicone (RTV; both by Henkel Corp, Düsseldorf, Germany). (The original products, the 30515 (GS) and the 30560 (RTV) have been superseded by Loctite 198819 and 270642, respectively.) The analogue was coated onto the socket and root surfaces with micro-brushes (Kerr Applicators, Part No. 24680, Kerr Corporation, Orange, CA, USA). The 2 parts were loosely fitted together, the alignment jig (**Fig.**

1F) was slipped over them, the upper setscrew was tightened against the crown and the 2 lower screws were lightly tightened in position. Two 1.0 mm spacers (0.04 inch diameter orthodontic wires) were inserted between the crown and the alveolar "bone". The 2 lower setscrews were fully tightened while the crown was pushed down and held tightly against the wires to form the 0.3 mm layer of the PDL analogue. The wires were removed, the excess material was wiped off with micro-brushes and the PDL was allowed to cure.

Testing set-up

With the maxillary assembly still attached to the testing apparatus, but the complete lower assembly (tooth/load cell) sitting freely on the table and the alignment jig (**Fig. 1F**) still tightened, the upper assembly was rested on the lower tooth, and the entire lower assembly was moved around slightly until the maxillary tooth "fell" into a stable centric Class I occlusion. The lower assembly was then securely clamped to the table. A carpenter square (generic), with 0.20 mm shims (Feeler Stock No. 667-8, L. S. Starrett Co., Athol, MA, USA) on both sides, was positioned tightly against the load cell's base plate, and then the square was clamped to the table for the duration of the experiment, **Figs. 1A** and **C**. In this way, the entire lower assembly could be precisely shifted away from centric into the (n =) 21 occlusal relationships, in all directions, by keeping the carpenter square fixed and replacing the shim combinations in 0.05 mm thickness increments, **Figs. 1A** and **C** and **Table 1**.

Testing

Once the parts were securely clamped, the maxillary tooth was manually lowered with the MTS onto the mandibular tooth until a slight slack was observed in the supporting chain. This indicated that the full bite force (F_z = ~20 N) was being exerted. This position of the MTS actuator was set as its zero point.

To investigate the expressions of PDL *creep* and *recovery*, instead of the previously used ramp bite-force displacement loading function, 3 different sets of step functions were applied, with 4 chomps of each. The step functions were 1 second on/4 seconds off, 2.5 seconds on/2.5 seconds off, and 4 seconds on/1 second off. The testing machine was set-up to run one of these 3 step load profiles in one of the 21 occlusal relationships (**Table 1**). The 4-chomp test was run with the setscrews (**Fig. 1F**) tightened (rigid attachment). Then, the setscrews were fully loosened (PDL attachment) and the 4-chomp test was repeated. The shims were then changed to one of the other 21 occlusal relationships and the test was run again. Then, with the setscrews tightened, the test was repeated, and so on for the remaining 19 configurations. The entire process was then performed using the 2 other step loading protocols. Thus, the entire experiment comprised a total of 504 (21 x 2 x 3 x 4) chomps.

Statistical Methods

With a sample size of 21 occlusal configurations (**Table 1**), the study had 80% power to detect an effect size of 0.886, assuming a 5% significance level for each test. The standard deviation of

the difference in $F_{lateral}$ creep is estimated to be 0.05 N, so the study was able to detect $F_{lateral}$ recovery differences of 0.045 N between groups.

Comparisons among the 4 chomps were made using repeated measures ANOVA, allowing a different variance for each chomp and varying correlations between chomps. Using data from chomp 2, comparisons between on/off times and between attachment types (rigid or PDL) were made using repeated measures ANOVA, allowing a different variance for each time-type combination and varying correlations between time-type combinations. A 5% significance level was used for all tests. Analyses were performed using SAS version 9.4 (SAS Institute, Inc., Cary, NC, USA).

Results

Note that italicized 4-digit numbers refer to one of the 3 loading protocols. Thus, *1040* is 1 second on and 4 seconds off, *2525* is 2.5 seconds on and 2.5 seconds off, while *4010* is 4 seconds on and 1 second off. A 4-digit plain text number refers to one of the 21 tested occlusal configurations, **Table 1**.

Of the 21 tested occlusal relationships, data are presented for the 4 (bolded in **Table 1**) that are furthest from centric (2020). In **Fig. 2**, the results are shown in the form of F_y (N) vs. F_x (N). Thus if an arrow is drawn from the origin to a point (F_x, F_y) on a curve, it represents the $\mathbf{F_{lateral}}$ force vector that acts on the lower tooth within the occlusal (x – y or linguobuccal – mesiodistal) plane, **Fig. 1C**. The dashed arrows in **Fig. 2A** illustrate such $\mathbf{F_{lateral}}$ force vectors.

Figure 3 shows some of the same data in the form of $F_{lateral}$ (N) vs. time (sec). Specifically, in each panel, the 1st and 4th chomps are compared under 2 loading conditions (**3A** vs. **3C** and **3B** vs. **3D**) and PDL vs. rigid (**3A** vs. **3B** and **3C** vs. **3D**).

Statistical analyses of the values for $F_{lateral}$ peaks showed that:

(1) There are chomp-to-chomp differences, $p < .001 – .038$, more so with the PDL. This is best seen in **Fig. 3**.
(2) PDL and Rigid were significantly different, $p < .001$, for all outcomes. This can be seen in **Figs. 2** and **3**.
(3) On times affected all PDL outcomes, $p < .044$. They also had an effect on Rigid "creep". This can be seen in **Fig. 3A** vs. **3C**.

Discussion

The Rigid/PDL combination represents occlusion between an implant-supported or ankylosed maxillary tooth and a natural mandibular tooth. The Rigid/Rigid results can be interpreted in terms of occlusion between implant-supported and/or ankylosed teeth. Although not a focus of this study, in concordance with a previous study, our results show that the implant/implant (Rigid/Rigid) contacts generate higher magnitude $\mathbf{F_{lateral}}$ forces than the implant/tooth (Rigid/PDL) pairs. Thus, by extrapolation, it is not unreasonable to conclude that tooth/tooth

(PDL/PDL) contacts would generate the smallest forces. These observations, and that the **$F_{lateral}$** directions also are affected, have major clinical and experimental implications.(deMoya, Schmidt et al. 2021)

One purpose of the step (vs. ramp) function (**Fig. 4**) was to improve the constancy/stability of the load application. The other purpose was to enable adjustability of the loading profile. The former was clearly achieved with the statistical analysis that showed that the step functions produced smaller variability than the ramp loading, **Table 2**. The explanation is as follows.

With the original ramp loading protocol, **Figs. 4A** and **B**, the weighted upper assembly was lowered onto and raised off of the lower crown in a prescribed ramp displacement mode at 0.2 Hz and 8 mm amplitude. To ensure that the full bite force was being applied, the MTS was used to manually lower the upper assembly until a slight slack developed in the supporting chain, **Fig. 1A**, and at that position, the hydraulic actuator displacement was zeroed. The amount of that eyeballed slack determined the relative lengths of the On (clenching) and Off (discluded) times. As illustrated, a relatively large slack, S1 (**Fig. 4A**), resulted in longer On (On1) and shorter Off (Off1) times than with a smaller slack, S2 (**Fig. 4B**). This was not an issue with rigid attachment, but if a VE (*i.e.*, time-dependent) component is involved, then the On (creep) and Off (recovery) periods should be better controlled.

Thus, an important aspect of this project was the implementation and testing of the step loading protocol, **Fig. 4C**. In contrast to the ramp, the diagram shows that the step On and Off times are relatively unaffected by an inconsistent chain slack, with the large slack (thick gray curve) and the small slack (thin dashed line).

The second major advantage of the step function, if a VE material is involved, is that it is possible to prescribe the On/Off times, as in this study, as (1 sec)/(4 sec), (2.5)/(2.5) and (4)/(1), **Fig. 4D**. In all runs, the On (full-load or clench) + Off (discluded) times summed to 5 (*i.e.*, 1 + 4, 2.5 + 2.5 or 4 + 1) seconds, while the assembly was lowered and raised in 0.2 seconds each, for a total of 5.4 seconds per chomp cycle (0.185 Hz).

The importance of timing with VE materials can be seen in **Fig. 3**, in which the 1st and 4th chomps with the 4040 occlusal configuration are compared. (As the VE effects are cumulative from chomp-to-chomp, for display purposes, the 1st chomp vs. 4th chomp comparisons accentuate the differences, or the lack thereof, compared to a comparison of consecutive chomps.) **Figure 3A** shows results for loading protocol *4010* (4 seconds on, 1 second off) on the PDL model. During the clench periods, *i.e.*, the 4-seconds of maximum bite force (F_z) applications, the material creeps. As a result of that creep, $F_{lateral}$ decreased in magnitude by the amount indicated by "Creep 1." During the subsequent 1-second off ($F_z = 0$) periods, the material started to return to its original dimensions (recovery), as reflected in the higher $F_{lateral}$ at the start of Chomp 4, and indicated by "Recovery." However, the 1-second recovery period was incomplete, resulting in a lower, by "Creep (residual)," peak $F_{lateral}$ in Chomp 4. Unlabeled, note also, by comparing square marker with square marker, the drop in the $F_{lateral}$ magnitude at the onset of disclusion. In contrast, as expected, loading protocol *1040* (**Fig. 3C**), with only 1 second for creep, but 4 seconds for recovery, exhibited a much smaller residual Creep.

Virtually no accumulating changes in $F_{lateral}$ are seen with the corresponding rigid attachments, **Figs. 3B** and **D**. And, in contrast to the PDL, the "creeps" are at their asymptotic limits. Furthermore, the rigid "creep" tends to be consistent in each chomp, and it is substantially smaller than the corresponding PDL creep. Critically, the rigid data exhibit total (elastic) recoveries with no evidence of viscous behavior. The rigid "creep" has been attributed to "stiction," an effect of fiction as the cusps settle in.(deMoya, Schmidt et al. 2021) It must be assumed that this phenomenon is also a component of the PDL results.

The chomp-to-chomp differences (statistical outcome 1 in Results and **Fig. 3**) and the PDL vs. Rigid differences (statistical outcome 2 and **Figs. 2** and **3**) essentially confirm, under more controlled loading conditions, the earlier results.(deMoya, Schmidt et al. 2021) Statistical outcome 3 (the effects of On/Off times, **Figs. 2** and **3**) demonstrates the need for prescribed controlled load timing when VE materials are involved. Thus, the main finding, illustrated in **Figs. 2D**, **3A** and **3C**, is that the loading schedule affects the magnitude and direction of the PDL analogue's $\mathbf{F_{lateral}}$. The effects of *4010*'s longer clench (creep) duration is evident **Fig. 2D**, however, the effects of its shorter recovery (discluded) period cannot be depicted in this graph. **Figures 3A** and **C**, however, do show the magnitude behaviors.

As the magnitudes of the $\mathbf{F_{lateral}}$ vector are sufficient to demonstrate statistical differences, there is no need to involve $\mathbf{F_{lateral}}$ direction in these analyses. However, note that the direction changes *throughout* a chomp (**Fig. 2**), particularly in the VE clench phases, **Figs. 2A** and **D**. Also noteworthy is the observation that the 4 demonstrated occlusal relationship offsets produce $\mathbf{F_{lateral}}$ force vector directions in all 4 quadrants, **Fig. 2**.

Conclusion

Although viscoelasticity is a complex phenomenon, its relatively simple expressions in occlusion mechanics should not be discounted.

Overall, the main determinant of $\mathbf{F_{lateral}}$ magnitude and direction is the occlusal relationship, **Fig. 2**. The difference between PDL and rigid depends on the occlusal scheme, **Figs. 2A** and **B**. As expected, loading schedule has minimal effect on rigid, **Fig. 2C**, but it does affect the PDL results, **Fig. 2D**. Thus, if a VE PDL is incorporated into the specimen, the loading profile should be well defined and controlled.

Disclosures

The authors have no conflicts of interest and only internal support was utilized.

References

Beninati, C. J. and T. R. Katona (2019). "The combined effects of salivas and occlusal indicators on occlusal contact forces." J Oral Rehabil **46**(5): 468-474.

Dawson, P. E. (2006). Functional occlusion: from TMJ to smile design. St. Louis, Mo, Mosby.

deMoya, A. V., E. R. Schmidt, G. J. Eckert and T. R. Katona (2021). "The effects of a periodontal ligament analogue on occlusal contact forces." J Oral Rehabil.

Harrel, S. K. and M. E. Nunn (2009). "The association of occlusal contacts with the presence of increased periodontal probing depth." J Clin Periodontol **36**(12): 1035-1042.

Helms, R. B., T. R. Katona and G. J. Eckert (2012). "Do occlusal contact detection products alter the occlusion?" J Oral Rehabil **39**(5): 357-363.

McCrea, E. S., T. R. Katona and G. J. Eckert (2015). "The effects of salivas on occlusal forces." J Oral Rehabil **42**(5): 348-354.

Mitchem, J. A., T. R. Katona and E. A. S. Moser (2017). "Does the presence of an occlusal indicator product affect the contact forces between full dentitions?" J Oral Rehabil **44**(10): 791-799.

Okeson, J. P. (2013). Management of temporomandibular disorders and occlusion. St. Louis, Mo, Elsevier Mosby.

Passanezi, E. and A. C. P. Sant'Ana (2019). "Role of occlusion in periodontal disease." Periodontol 2000 **79**(1): 129-150.

ScienceDirect. (2019a). "Viscoelasticity." Retrieved October 3, 2019, 2019, from https://www.sciencedirect.com/topics/chemistry/viscoelasticity.

ScienceDirect. (2019b). "Viscoelastic Behavior." Retrieved November 1, 2019, 2019, from https://www.sciencedirect.com/topics/materials-science/viscoelastic-behavior.

Xia, Z. and J. Chen (2013). "Biomechanical validation of an artificial tooth-periodontal ligament-bone complex for in vitro orthodontic load measurement." Angle Orthod **83**(3): 410-417.

Yang, S.-M. and H.-J. Chung (2019). "Three-dimentional finite element analysis of a mandibular premolar with reduced periodontal support under a non-axial load." Oral Biology Research **43**: 313-326.

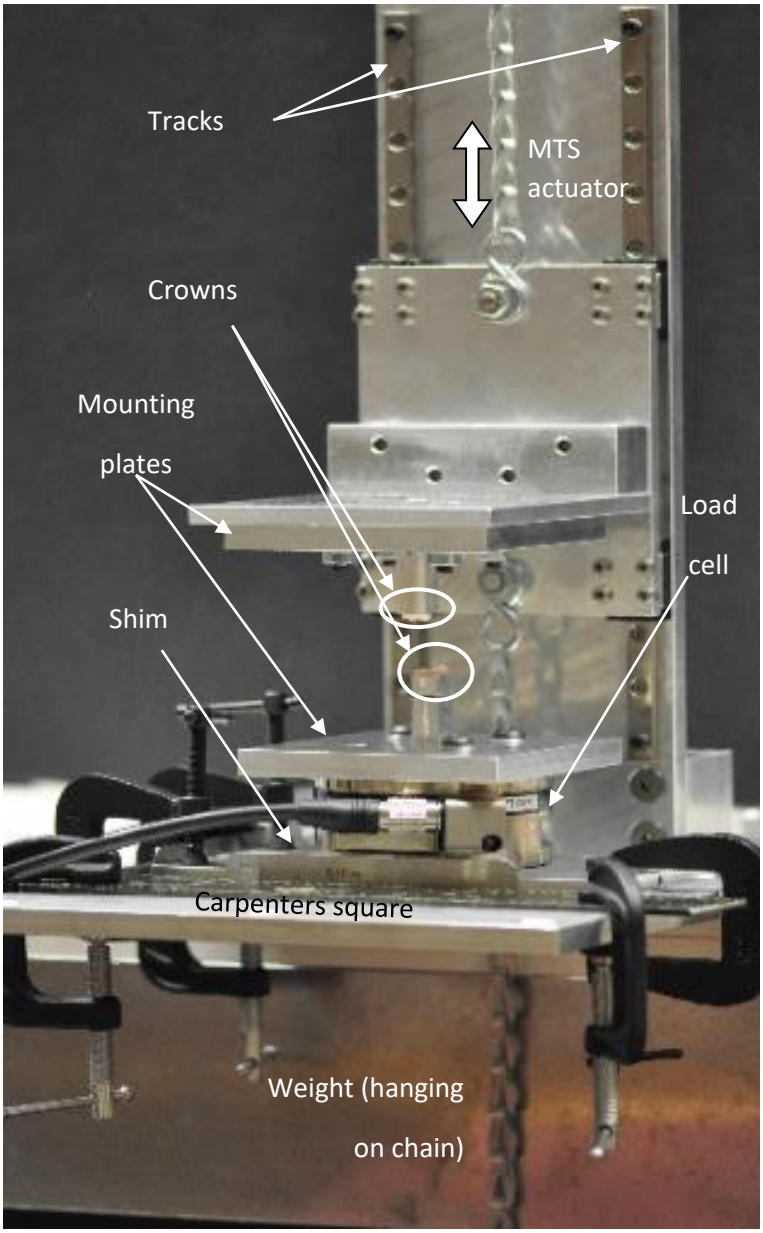

(1A)

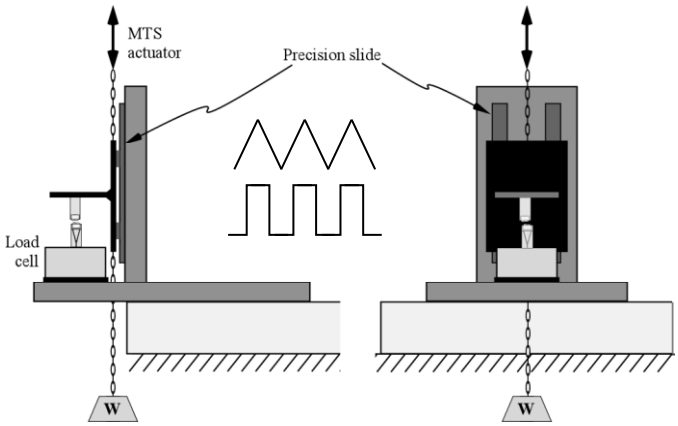

(1B)

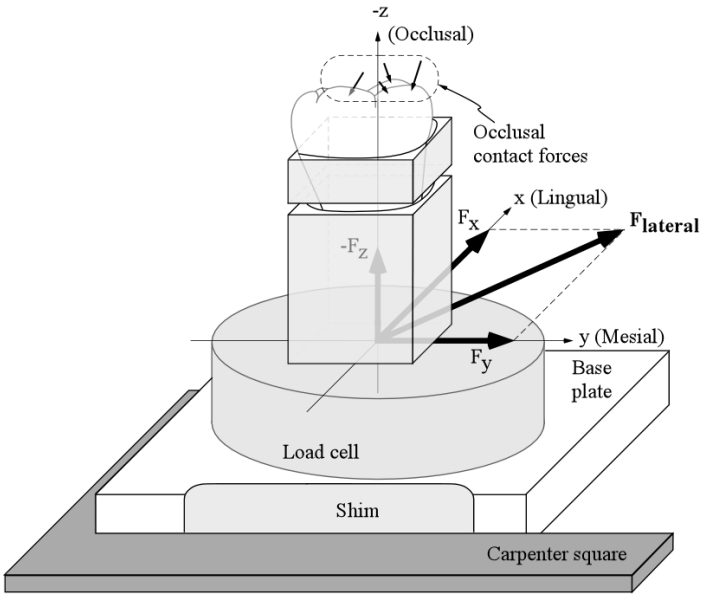

(1C)

FIGURE 1 (**A** and **B**) Picture and schematics of testing apparatus. **B** also illustrates the actuator's prescribed ramp (top) and step (bottom) displacement functions. (**C**) F_x, F_y and F_z are applied (and measured) by the load cell to maintain the lower tooth in equilibrium as the individual contact forces act on the occlusal surface.

$$F_{lateral} = \sqrt{F_x^{\,2} + F_y^{\,2}}\ .$$

(**D**) Aluminum maxillary tooth (left), mandibular tooth/socket assembly (center) and assembled mandibular crown/bone (right). (**E**) Given the specifications for the root (30° and 8 mm diameter at the CEJ), calculations were performed such that the 1.0 mm wire spacers would produce the 0.3 mm PDL space. (**F**) Occlusal and side view schematics and pictures of the PDL polymerization alignment jig. Two 0.04 inch (= 1.02 mm) diameter orthodontic wires act as the spacers, (**E**). The same jig (without the wires) also serves as the rigid attachment when the 3 set screws are tightened, and as the PDL set-up when the 3 screws are fully loosened.

(1D)

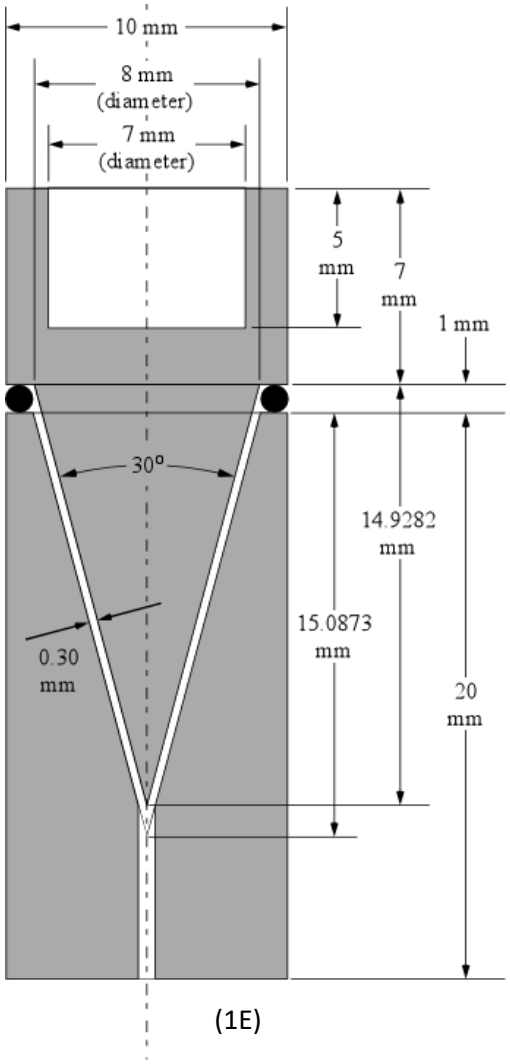
10 mm
8 mm
(diameter)
7 mm
(diameter)
5
mm
7
mm
1 mm
30°
14.9282
mm
15.0873
mm
0.30
mm
20
mm

(1E)

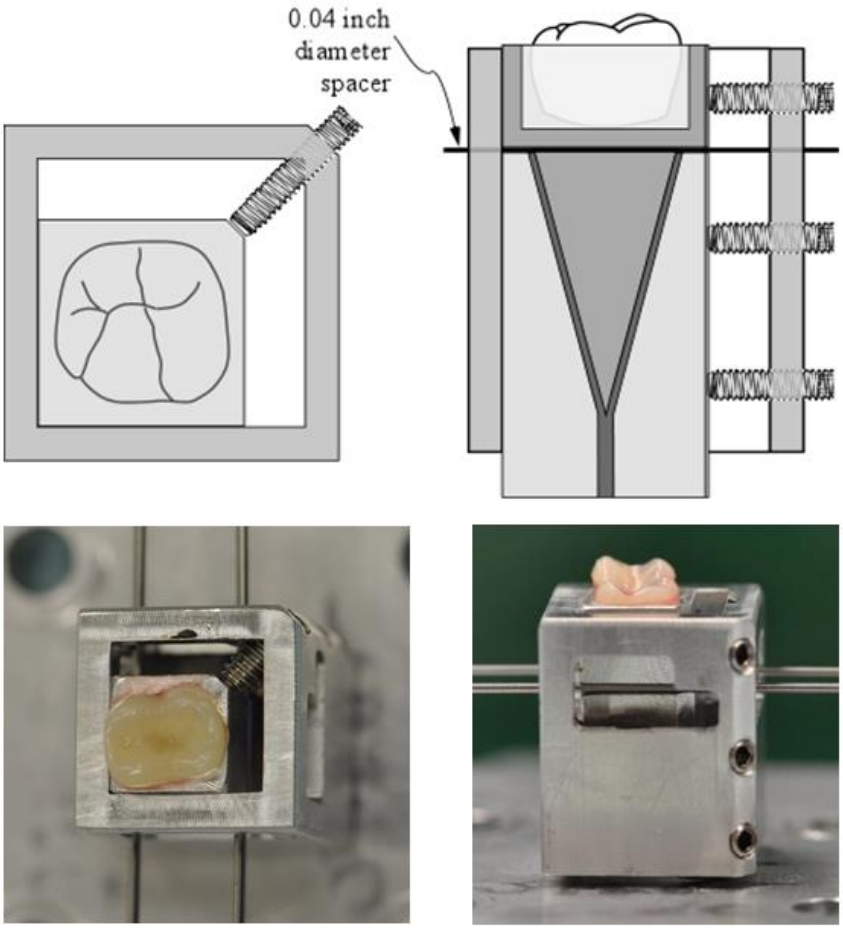
0.04 inch
diameter
spacer

(1F)

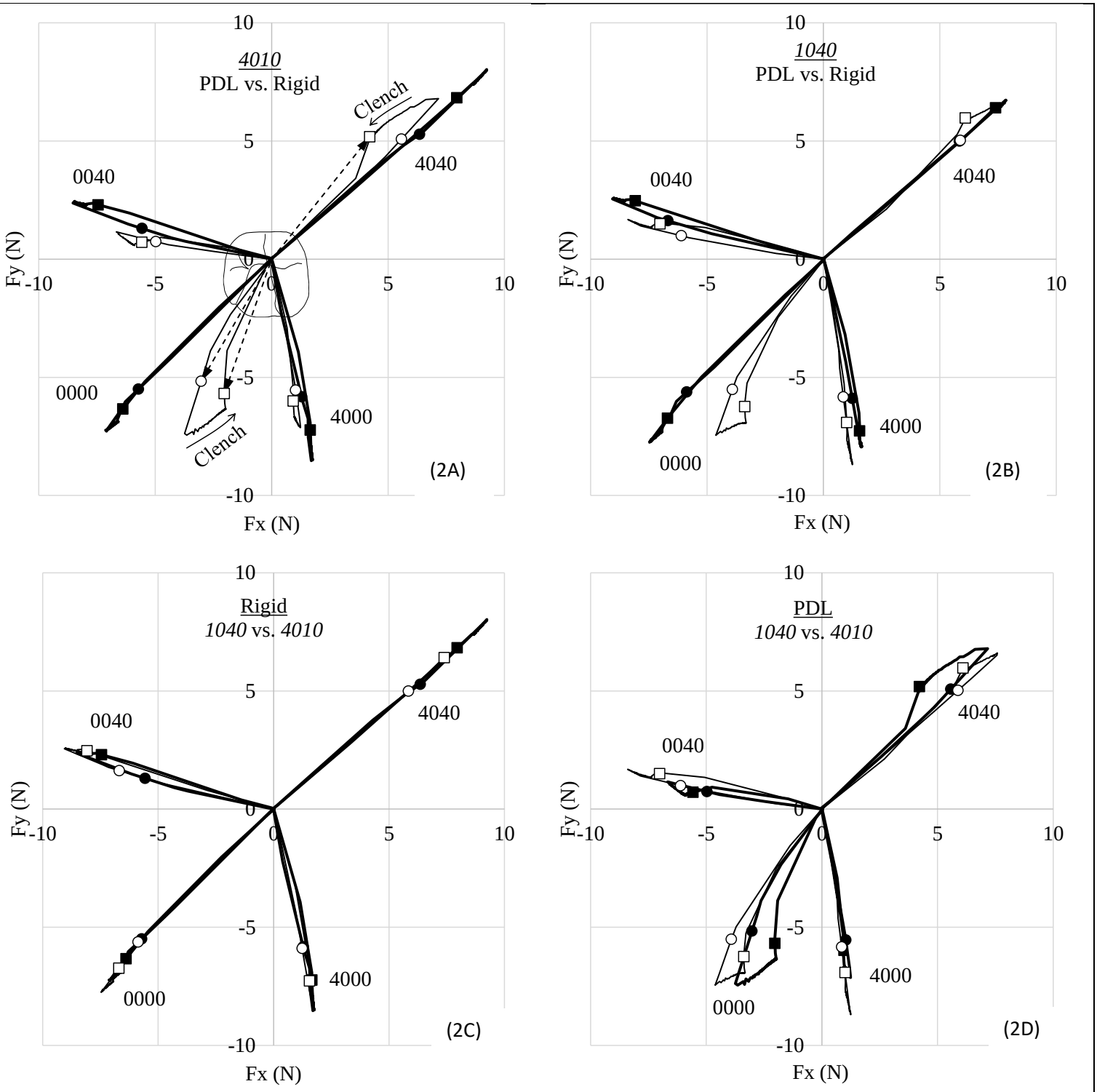

FIGURE 2 F_y (N) vs. F_x (N) for the 2nd chomp of occlusal configurations furthest (0.28 mm) from centric, 0040, 4040, 4000 and 0000. Circles and squares represent occlusal and disclusal values, respectively, corresponding to the bite force, F_z = 15 N. In (**A**) (loading protocol *4010*) and (**B**) (protocol *1040*), PDL and rigid results are depicted by, respectively, thin lines with open symbols and thick lines with solid symbols. In (**C**) and (**D**), rigid and PDL attachment, respectively, the thin lines and open symbols are for the *1040* loading protocol and the thick lines with solid symbols are for the *4010* loading. Dashed arrows in (**A**) are examples of $\mathbf{F_{lateral}}$ force vectors produced by 15 N bite forces.

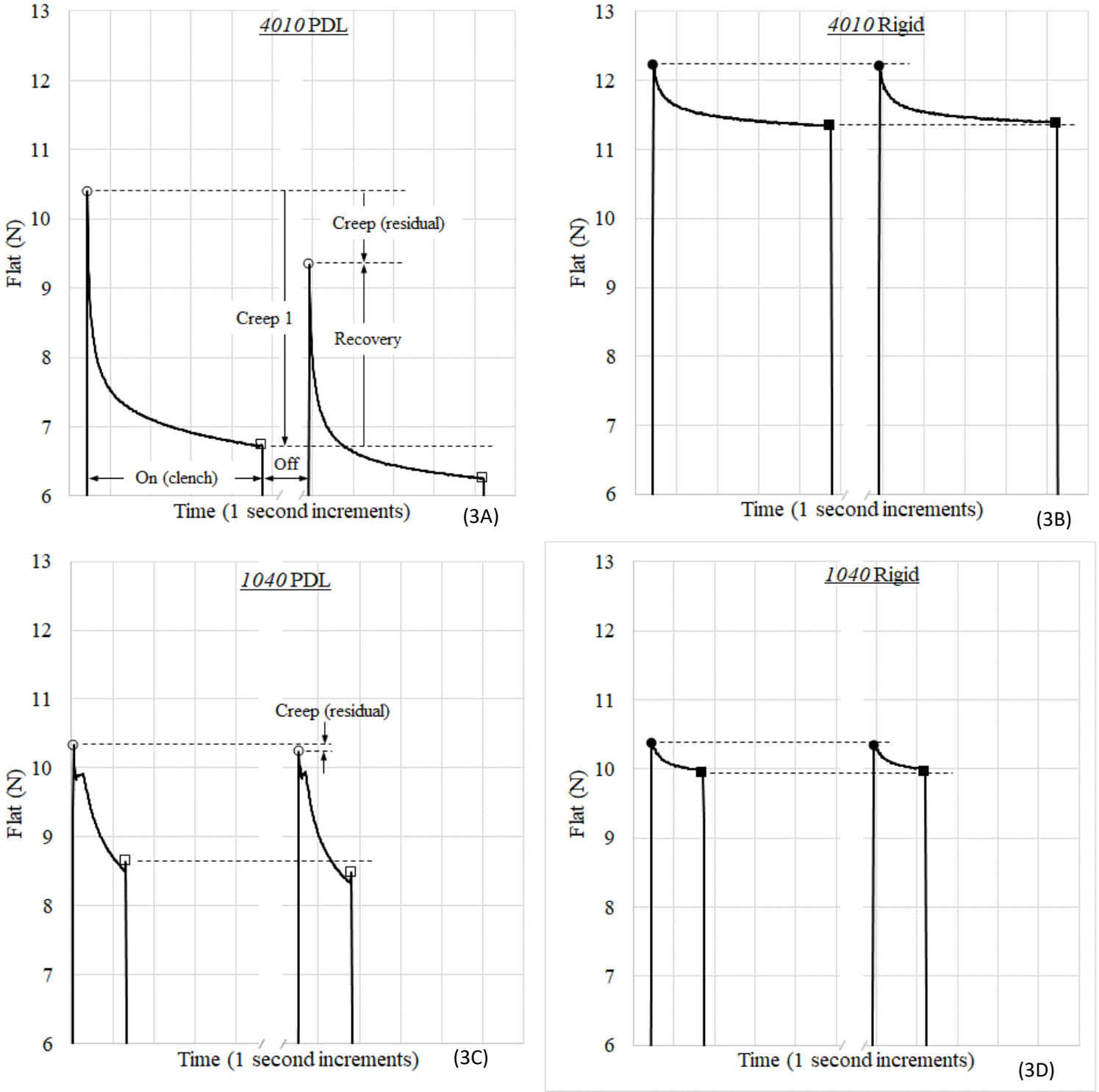

FIGURE 3 F_{lat} (N) vs. Time (sec) comparing the 1st and 4th chomps of configuration 4040. (**A** and **B**) Loading profile *4010* for the PDL and rigid attachments, respectively. (**C** and **D**) Similarly, for loading profile *1040*. Circles indicate the transition point from occlusion to clenching. Squares demarcate the end of clenching and the start of disclusion.

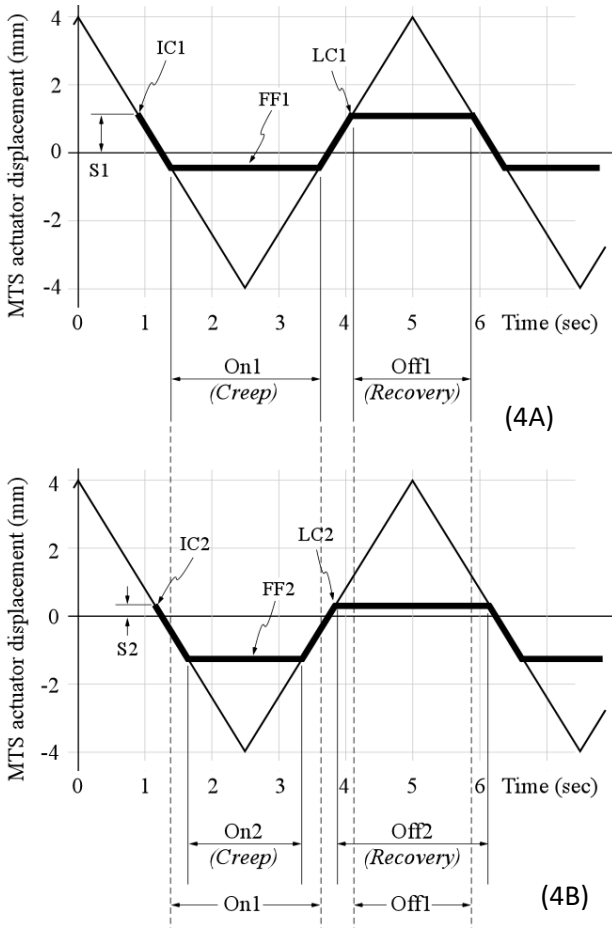

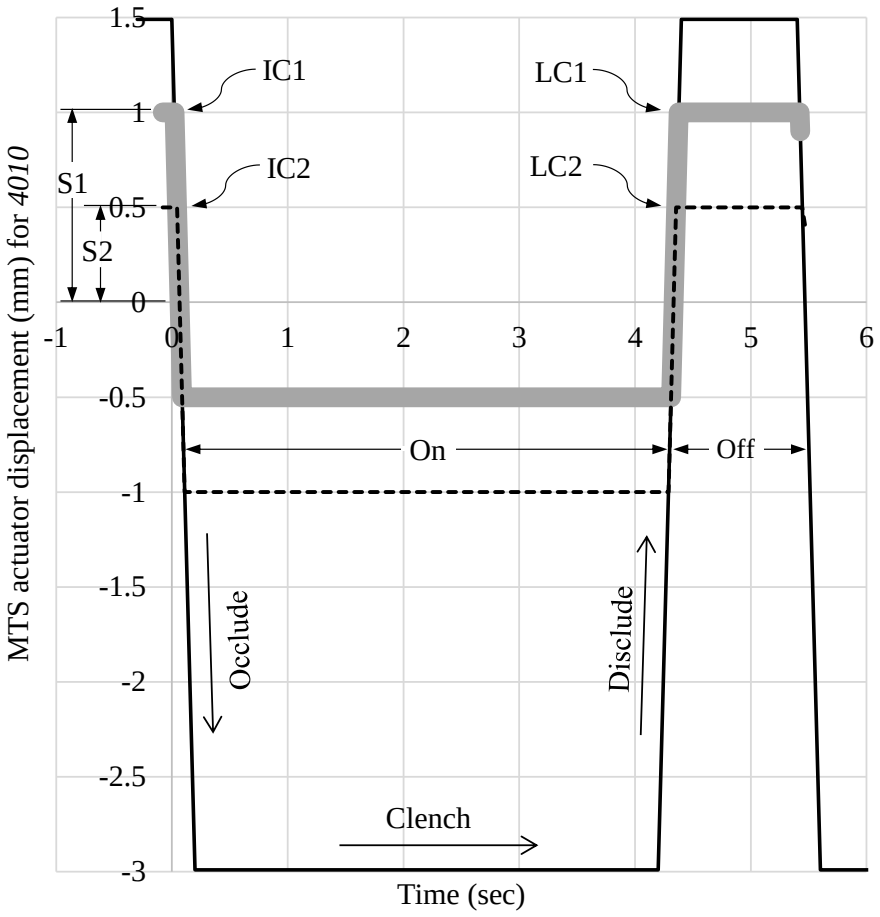

IC: Initial contact
FF: Full force (clench)
LC: Last contact
S: Slack in supporting chain

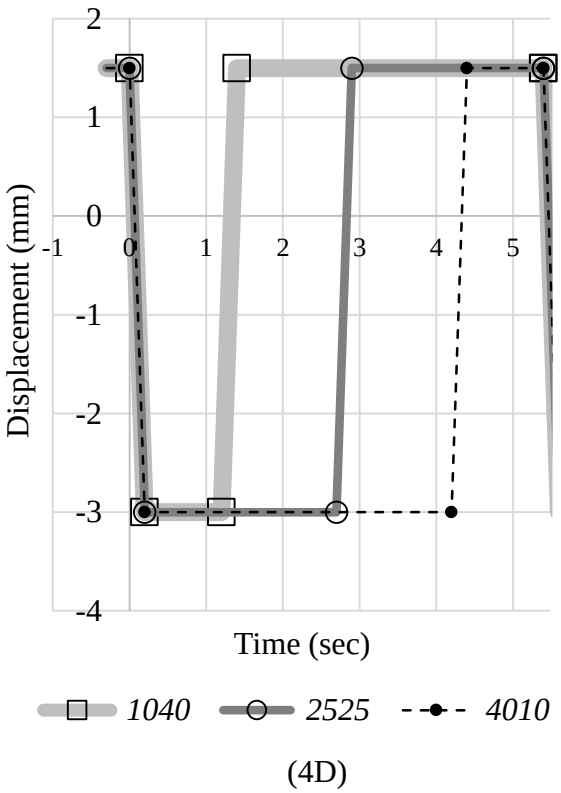

(4D)

FIGURE 4 MTS (**Fig. 1**) actuator-prescribed displacement profiles. (**A**) and (**B**), ramp displacement mode at 0.2 Hz and 8 mm amplitude used in previous investigations. (**A**) shows the effects on the On (clench) and Off times of a large slack (S1) in the supporting chain. Similarly, (**B**) shows the effects of a smaller slack, S2. IC → FF is "occlude," FF is clenching and FF → LC is "disclude". (**C**) With a step function, the On and Off times are relatively unaffected by the inconsistency in chain slack with the large (thick gray curve) and the smaller (thin dashed line) slack. (**D**) shows the 3 loading profiles used in this study with (1 sec)/(4 sec), (2.5)/(2.5) and (4)/(1) On/Off times, denoted, respectively, by *1040* (thick gray line), *2525* (thin gray line) and *4010* (dashed line).

Table 1: Nomenclature for the 21 relative positions of the mandibular assembly established with the 0.05 mm incremental shims, **Fig. 1A**. The nomenclature is in the form yyxx where yy and xx correspond to the thicknesses of the shims in mm x 100. Thus, the 0040 is 0.20 mm lingual and 0.20 mm distal to centric (2020), which is in the middle at (0.20, 0.20). Results for the 4 bolded configurations are shown in **Fig. 2**.

x (lingual)

0040								**4040**
	0535						3535	
		1030				3030		
			1525	2025	2525			
			1520	2020	2520			
			1515	2015	2515			
		1010				3010		
	0505						3505	
0000								**4000**

y (mesial)

Table 2: Time (sec) between occlusion and disclusion at F_z = 15N. Levene's test for homogeneity of variances showed that ramp loading had higher variability (p=0.001) than the step functions.

		Occlusal relationship (**Table 1**)				
		0040	4040	0000	4000	
Loading	Attachment	Time (sec)				
1040 Step	Rigid	1.28	1.29	1.28	1.29	
	PDL	1.27	1.28	1.28	1.35	
	Avg (R & P)					1.29
4010 Step	Rigid	4.31	4.33	4.28	4.28	
	PDL	4.29	4.31	4.31	4.29	
	Avg (R & P)					4.30
Ramp*	Rigid	2.87	2.96	3.01	2.85	
	PDL	2.75	2.50	2.84	2.82	
	Avg (R & P)					2.83

*deMoya, A. V., E. R. Schmidt, G. J. Eckert and T. R. Katona (2021). "The effects of a periodontal ligament analogue on occlusal contact forces." J Oral Rehabil.